

# Investigating the phytoplankton diversity in the Great Calcite Belt: perspectives from hyper- and multi-spectral satellite retrievals and numerical modeling



Svetlana N. Losa<sup>1</sup>, Julia Oelker<sup>2</sup>, Mariana A. Soppa<sup>1</sup>, Martin Losch<sup>1</sup>, Stephanie Dutkiewicz<sup>3</sup>, Tilman Dinter<sup>1</sup>, Andreas Richter<sup>2</sup>, Vladimir Rozanov<sup>2</sup>, John P. Burrows<sup>2</sup>, Astrid Bracher<sup>1,2</sup>



<sup>1</sup>Alfred Wegener Institute Helmholtz Centre for Polar and Marine Research, Bremerhaven, Germany

<sup>2</sup>Institute of Environmental Physics (IUP), University of Bremen, Bremen, Germany

<sup>3</sup>Massachusetts Institute of Technology, Cambridge, Massachusetts, USA

oelker@iup.physik.uni-bremen.de; svetlana.losa@awi.de

## Abstract

This study highlights benefits and challenges of applying coupled physical/biogeochemical modeling and the synergistic use of different satellite retrieval algorithms for investigating the phytoplankton diversity in the Great Calcite Belt. This area is of great interest for understanding biogeochemical cycling and ecosystem functioning under present climate changes observed in the Southern Ocean. Our coupled model simulations of the phenology of various Phytoplankton Functional Types (PFTs) are based on a version of the Darwin biogeochemical model (Dutkiewicz et al., 2015) coupled to the MITgcm circulation model (MITgcm Group 2012), where both - the physical and biogeochemical modules - are adapted for the Southern Ocean. As satellite-based PFT information, we consider products of the PhytoDOAS (Bracher et al. 2009, Sadeghi et al. 2012) using SCIAMACHY and OMI hyper-spectral optical satellite measurements. We also address aspects of combining this information synergistically (SynSenPFT, Losa et al. 2017) with the phytoplankton composition retrieved with OC-PFT (Hirata et al. 2011, Soppa et al. 2014, 2016) based on multi-spectral optical satellite data (OC-CCI) and obtained by numerical modelling to allow for long time-series on the Southern Ocean phytoplankton diversity. To evaluate the satellite retrievals and model simulations we use *in situ* PFTs obtained a diagnostic pigment analysis (Soppa et al., 2017) as well as by scanning electron microscopy (Smith et al., 2017).

## Satellite Observations: The Great Calcite Belt

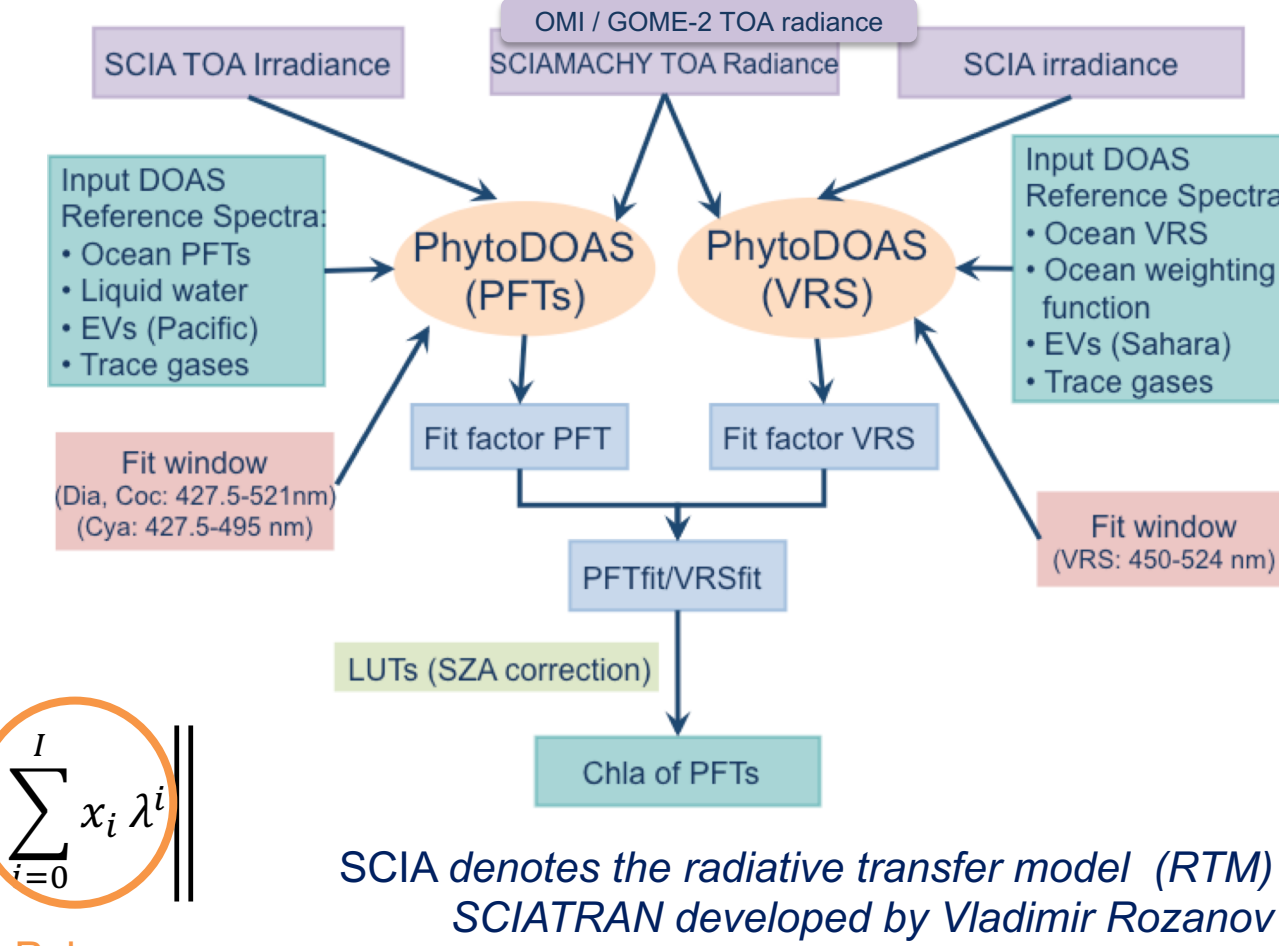
### Comparison of different hyper-spectral sensors

Chlorophyll "a" of PFTs in the Southern Ocean are extracted using differential optical absorption spectroscopy (PhytoDOAS, Bracher et al. 2009, Sadeghi et al. 2012, Bracher et al. 2017: doi.org/10.1594/PANGAEA.870486) on hyperspectral satellite data.

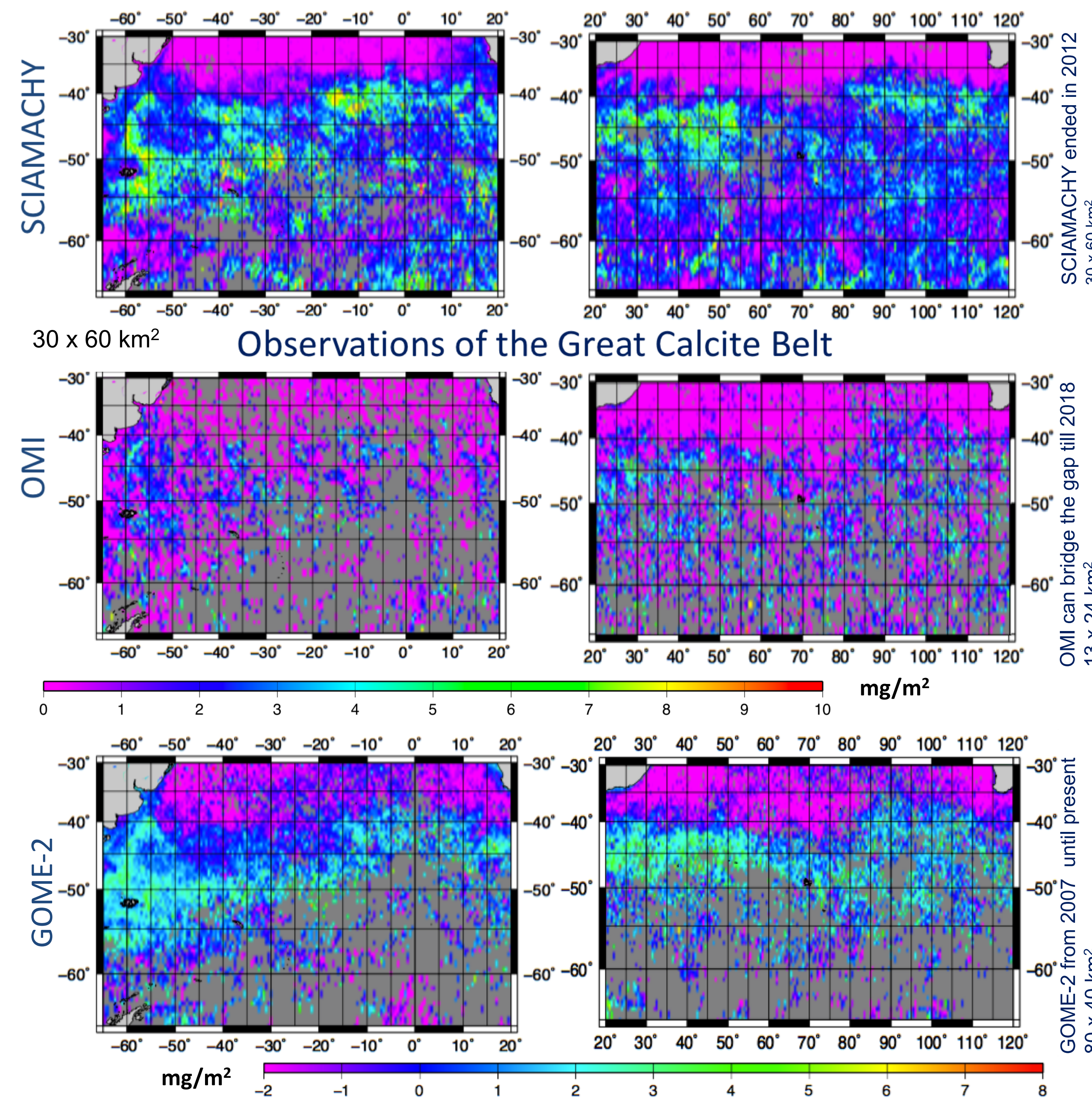
$$I(\lambda) = I_0(\lambda) \cdot e^{-\tau(\lambda)} \Rightarrow \tau(\lambda) = \ln \left( \frac{I_0(\lambda)}{I(\lambda)} \right)$$

$$S_{VRS}, S_j = \text{Arg min} \left\| \tau(\lambda) - \left( \sum_{k=1}^K S_k \sigma_k(\lambda) + \sum_{l=1}^L S_l a_l(\lambda) - S_{VRS} v(\lambda) - S_{r1} r_1(\lambda) \right) \right\|$$

Atmosphere Phytoplankton Inelastic scattering (VRS), Polynom



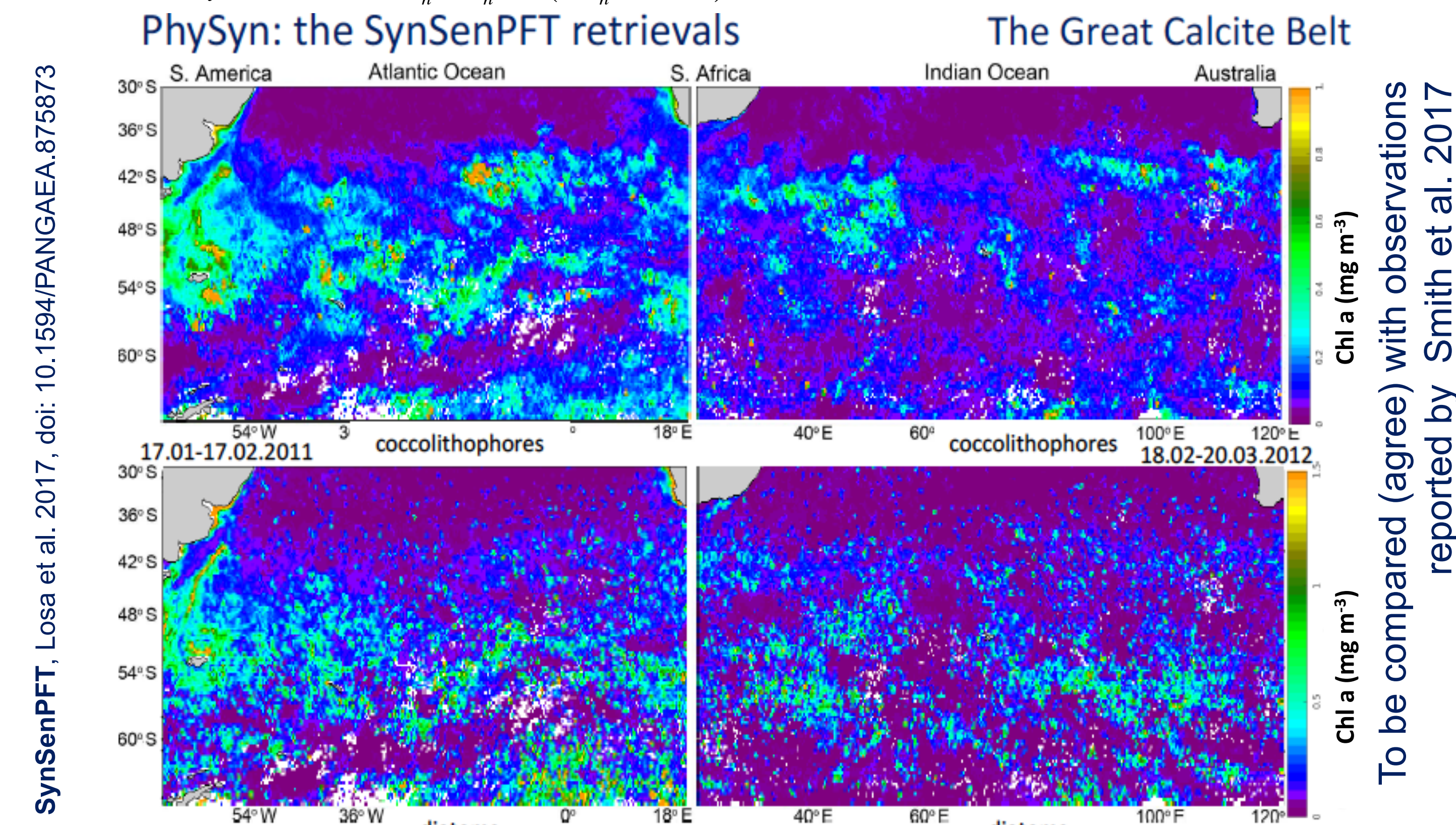
### SCIAMACHY vs. OMI PhytoDOAS coccolithophores retrievals



Despite the OMI sensor degradation and large ground pixel size of GOME-2, the information merged from these hyperspectral sensors and assimilated with SynSenPFT (Losa et al. 2017) would allow to bridge the current and future satellite missions.

### Synergistic Product: Combining hyper- and multi-spectral satellite data

$$x^a = x^b + K(y - Hx^b) \quad K_n = P_n^b H^T (HP_n^b H^T + R)^{-1}$$



References: Bracher, A. et al. (2009). Quantitative observation of cyanobacteria and diatoms from space using PhytoDOAS on SCIAMACHY data. *Biogeosciences*, 6, 751-764. Bracher, A. et al. (2017). Global monthly mean chlorophyll "a" surface concentrations from August 2002 to April 2012 for diatoms, coccolithophores and cyanobacteria from PhytoDOAS algorithm version 3.3 applied to SCIAMACHY data. <https://doi.org/10.1594/PANGAEA.870486>. Dutkiewicz, S. et al. (2015). Capturing optically important constituent and properties in a marine biogeochemical and ecosystem model. *Biogeosciences*, 12, 4447-4481. Follows et al. (2007). Emergent Biogeography of Microbial Communities in a Model Ocean. *Science*, 315, 1843-1846. Longhurst, A. (1998). *Ecological Geography of the Sea*. Academic Press. Losa, S. N. et al. (2017). Synergistic Exploitation of Hyper- and Multi-Spectral Precursor Sentinel Measurements to Determine Phytoplankton Functional Types (SynSenPFT). *Frontiers in Marine Science*, 4(202), 22 pp. Losa, S. N. et al. (2017). Global chlorophyll "a" surface concentrations for diatoms, coccolithophores and cyanobacteria as the synergistic SynSenPFT product combined PhytoDOAS and OC-PFT for the period of time August 2002 - April 2012. <https://doi.org/10.1594/PANGAEA.875873>. Menemenlis, D. et al. (2008). High resolution global ocean and sea ice data synthesis (2008) *Mercator Ocean Quarterly Newsletter*, 31, 13-21. Sadeghi, A. et al. (2012). Improvement to the PhytoDOAS method for identification of coccolithophores using hyper-spectral satellite data. *Ocean Science*, 8, 1055-1070. Soppa, M. A. et al. (2014). Global Retrieval of Diatom Abundance Based on Phytoplankton Pigments and Satellite Data. *Remote Sensing*, 6(10), 10089-10106. Soppa, M. A. et al. (2016). Diatom Phenology in the Southern Ocean: Mean Patterns, Trends and the Role of Climate Oscillations. *Remote Sensing*, 8(420), pp. 1-17. Soppa, M. A. et al. (2017). Global chlorophyll "a" concentrations for diatoms, haptophytes and prokaryotes obtained with the Diagnostic Pigment Analysis of HPLC data compiled from several databases and individual cruises. doi:10.1594/PANGAEA.875879.

## Modeling

The biogeochemical module, among 42 biogeochemical compartments ( $c_i$ ), describes 6 various phytoplankton functional types: analogues of (large) diatoms, other micro-phytoplankton, prochlorophytes, other pico-phytoplankton (including small diatoms), nitrogen fixing phytoplankton and coccolithophores (as nano-phytoplankton with corrected physiology to account for high affinity for nutrients and ability to escape grazing control).

$$\frac{\partial}{\partial t} c_i - \nabla \cdot (K_h \nabla c_i) + \nabla \cdot (V c_i) - \frac{\partial}{\partial z} \left( K_v \frac{\partial c_i}{\partial z} \right) = B_i$$

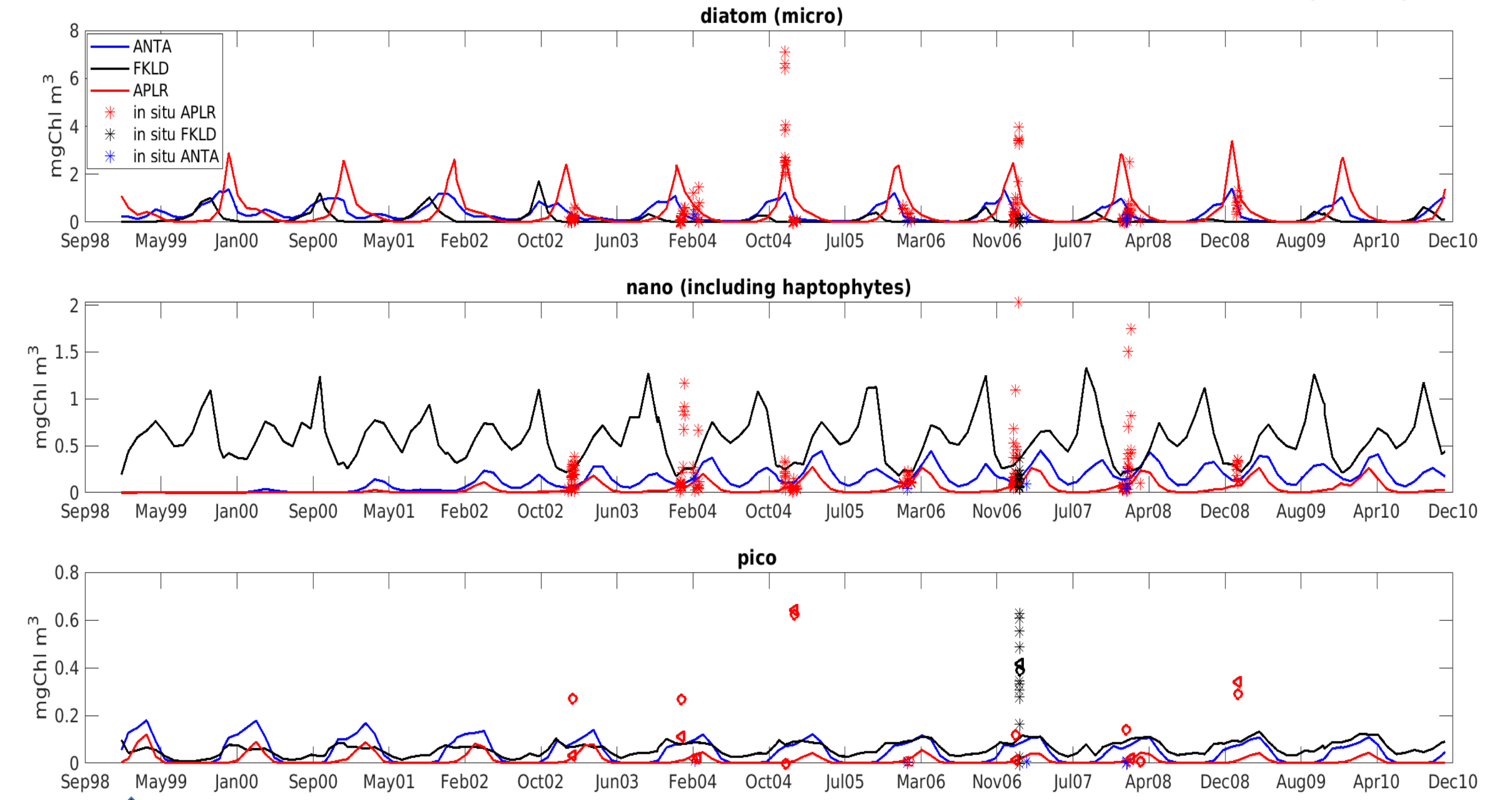


Figure 1: Model temporal evolution of PFTs chlorophyll "a" concentrations for 3 biogeochemical provinces (Longhurst, 1998): Antarctic Province (ANTA), Austral Polar Province (APLR) and Southwest Atlantic Shelves Province (FKLD). In-situ validation data: Soppa et al. 2017, doi:10.1594/PANGAEA.875879.

### Phytoplankton dominance

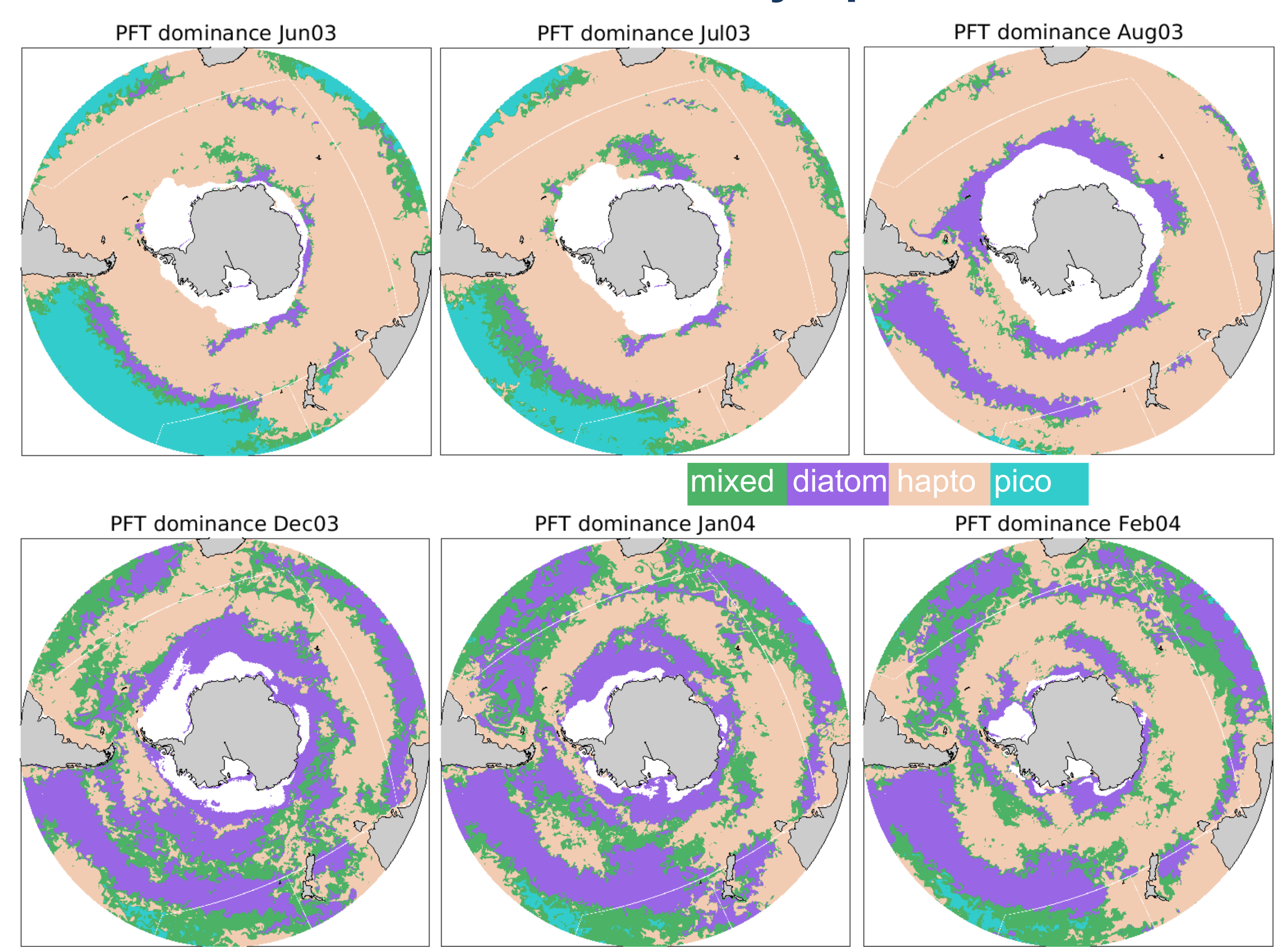


Figure 2: PFT dominance simulated with Darwin-MITgcm for January 2004, which is in agreement with the PFT dominance provided by PHYSAT satellite data product (<http://log.cnrs.fr/Physat-2/?lang=fr>). Pico represents *Prochlorococcus*.

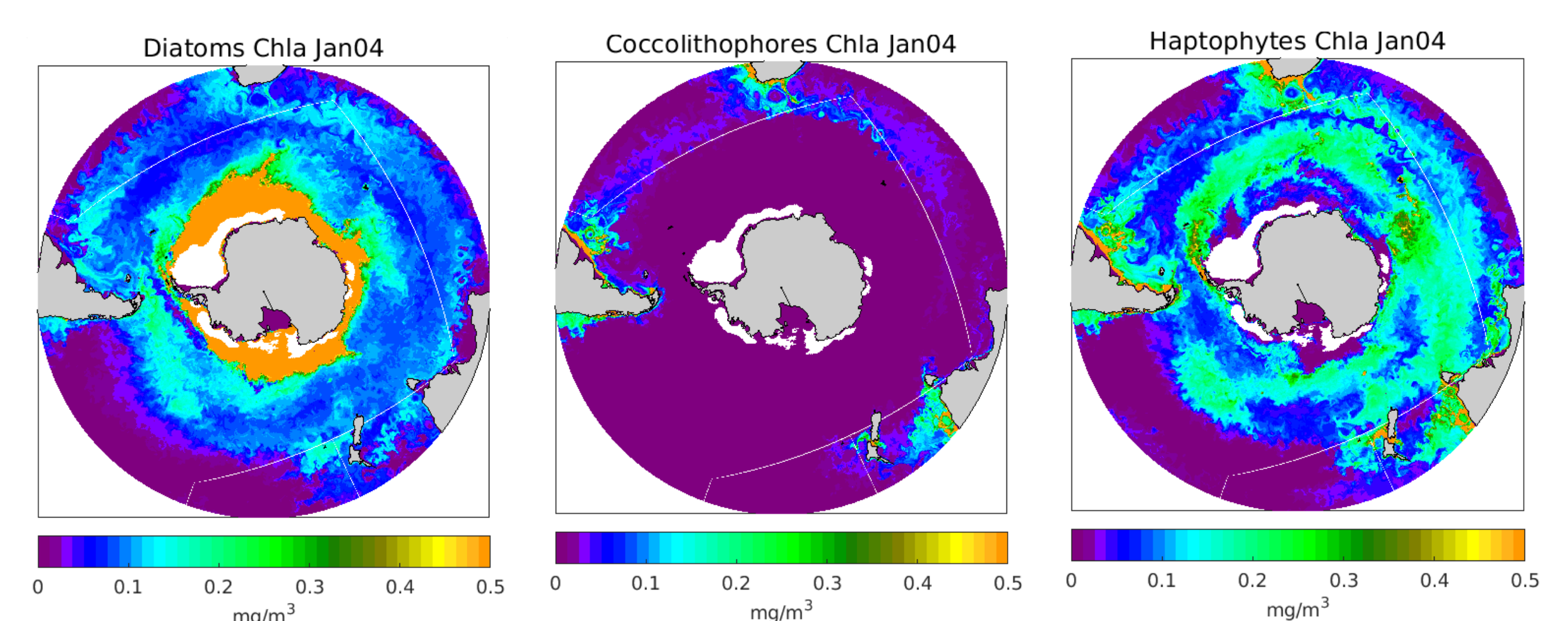


Figure 3: Spatial distribution (covering the GCB) of the model diatoms, haptophytes (including coccolithophores and *Phaeo*) Chlorophyll "a" concentration for January 2004.

Plausible simulations require(d) to introduce two size classes for diatoms, as two different model variables, and two distinct life stages of *Phaeocystis ant.* (colonies and solitary cells).

**Acknowledgement:** The coupled model simulations were performed with resources provided by the North-German Supercomputing Alliance (HLRN)

